

Low Temperature Oxidation Reaction of Microporous Carbons

J. K. Floess, S. A. Oleksy, and K. J. Lee
Department of Chemical Engineering
University of Illinois at Chicago
Chicago, IL 60680

Introduction

The oxidation of carbon by different gases is a reaction of major industrial importance, which to date at least, is not adequately understood on a molecular basis. Although a number of investigators¹⁻⁴ have proposed mechanistic models involving elementary steps for the gasification of carbon by different reactants, these models are generally qualitative in nature since the assignment of values to all individual rate constants is not yet possible. Careful experimental studies, in particular with graphite have been central to the development of these models and have been important in determining the role of certain postulated steps in the mechanisms. Other studies using labeled gas species have been useful in selecting the correct reaction pathway among possible alternative steps. Transient kinetic studies, in other instances, have led to a further understanding of the role of the intermediate complexes during reaction. However, a consensus on a reaction mechanism, particularly for the oxygen reaction, has yet to be obtained, nor have adequate quantitative comparisons been made between models and data obtained with various carbons.

In this study, work has focused on three aspects of the low temperature (<850K) carbon-oxygen reaction: the relationship between oxygen partial pressure and rate, the role of the surface oxide intermediate in the reaction mechanism, and the effect of carbon structure on the kinetics.

Experimental Equipment and Procedure

Rate data for both oxygen chemisorption and carbon gasification were obtained from measurements of weight gain (or loss) using a Stanton Redcroft thermogravimetric analyzer. The instrument consists of an electronic balance and a water cooled micro-furnace having a temperature limit of 1500°C and a heating rate capability of 50°C/min. A significant feature of the instrument is the small volume of the furnace (ca. 5 cc), which makes it possible to obtain a rapid change in gas composition upon introduction of a reactant. With nominal gas flowrates of 1 to 4 cc/s, the transient time for a change in gas composition is a few seconds. The TGA was also modified for operation under vacuum, which allows a further reduction in the transient time by allowing for slightly higher gas velocities in the furnace.

Weight changes of less than 1 μg can be readily measured with this instrument, and for a sample weight of 10 mg, this gives a weight gain or loss sensitivity of ca. 100 ppm (g/g carbon) after corrections for background weight changes caused by buoyancy and drag forces on the sample pan and hang down wire have been made. The actual amount of sample used in individual runs was modulated as necessary to minimize the effects of external heat transfer between the sample pan and the furnace and mass transfer between the sample and gas on the kinetics. This required rates to be nominally

held below 0.2 mg/min.

The experimental procedure was usually as follows. The sample was heated in nitrogen to 800°C at a rate of 50°C/min and held at 800°C for 3 min. This ensured the removal of the majority of the surface oxides. After outgassing, the sample was cooled to the reaction temperature and the experiment started by switching to the reactant gas. In several experiments, however, the carbon was first partially reacted at 535°C in air to 35% conversion and then reheated to 800°C before the start of an experiment. The total weight loss of the sample after burn-out and outgassing was 48%. At the conclusion of a run, the gas was switched back to nitrogen, the sample reheated to 800°C, and again cooled to the reaction temperature, where the sample weight was measured. The amount of oxygen on the carbon surface was calculated from the weight loss during outgassing as follows:

$$w_a = w_d(8+4\lambda)/(11+7\lambda) \quad (1)$$

where w_a is the weight of adsorbed oxygen, w_d is the measured weight loss, and λ is the CO/CO₂ mole ratio of the desorption products. The difference between the weight of oxygen in the desorption products and the total weight change in each run gives the amount of carbon gasified. This method was used in all experiments to separate the total weight change into an oxygen adsorption curve and a true carbon loss curve.

The carbon used in these experiments was Spherocharb, a molecular sieve carbon commercially available from Analabs, North Haven, CT. The elemental and physical analyses of the carbon are given in Table 1. Surface area data as a function of conversion were obtained from data reported by Hurt et al.⁵ The micropore diameter was estimated in two ways. One method used isosteric heat of adsorption data⁶ from physisorbed N₂ to estimate the pore size using theoretical adsorption potential models for a graphite surface⁷⁻⁸. The other technique used the random pore model⁹ to determine an average pore size from the micropore surface area and volume measurements. The former value is probably characteristic of the spacing between parallel orientated lamellae in a microcrystallite, whereas the latter represents an overall average ratio of pore volume to surface area. The difference of a factor of three in the calculated pore sizes indicates that there is a distribution of micropore sizes in the char.

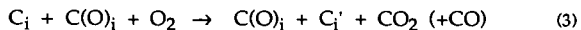
Results and Discussion

A. Oxygen Chemisorption and Reaction. Gravimetric measurements of the oxygen-carbon reaction rate have been made at 498, 548, 563, and 708 K with both the partially reacted and unreacted Spherocharb. Figure 1 shows the oxygen adsorption and carbon gasification curves obtained at 563K. For each experimental point, the reaction was stopped at appropriate times by switching to nitrogen, and the carbon outgassed to determine the oxygen content. The measured weight change was separated into individual curves for carbon loss and oxygen adsorption using a value of ∞ for λ in equation (1). No appreciable weight loss occurred when the reaction was stopped by switching to nitrogen; the surface oxides are stable and remain on the carbon at temperatures below ~900K. The initial oxygen adsorption rate is rapid (the characteristic reaction time is ~10s at 548K) and is characterized by an activation energy of a few kcal. A rapid loss of carbon, which is presumably due to the gasification of labile carbon atoms¹⁰, occurs concurrently with the initial uptake of oxygen. The initial rate of oxygen adsorption is more clearly shown by the data given in Figure 2, where adsorption data

between 3s and 300min are shown on an Elovich plot. This plot gave the best linear fit for the chemisorption data obtained in these experiments, implying that the adsorption sites are heterogeneous as would be expected.

At carbon conversions between 5 and 8%, the rate of carbon loss approaches a steady state value as shown by the carbon conversion curves presented in Figure 3 for data obtained at 708K. The oxygen content of the char (also shown in Figure 3), however, continues to increase with conversion, gradually reaching a value of ~0.18 mol O/mol C-remaining. The increase in oxygen content with conversion is more clearly shown in Figure 4, in which the oxygen to carbon ratio of the char is plotted as a function of carbon conversion for different reaction conditions. The amount adsorbed at equivalent conversions is practically the same for all reaction conditions, implying that the formation of the secondary oxides (as compared to those oxides formed initially) is a consequence of the removal of carbon from the solid substrate. Carbon reactivity was found to correlate with the initial amount of oxygen adsorbed but did not correlate with the variation in oxide concentration with conversion. A turn-over number (ton) based on the initial amount of oxygen adsorbed of $6.1 \times 10^{-3} \text{ sec}^{-1}$ was calculated for (unreacted) Spherocarb at 773K and 0.1 atm pressure. This value is in good agreement with the t.o.n. reported by Ahmed and Back¹¹ for a pyrolytic carbon.

B. Reaction Mechanism. Figure 5 shows the variation in rate with oxygen partial pressure. A value of 0.75 ± 0.06 was calculated for the reaction order with respect to oxygen from these data. The significant feature of these measurements, though, is the insensitivity of both the reaction order as well as the overall activation energy (not shown) to variations in oxygen partial pressure of almost two orders of magnitude and to variations in temperature of almost 150 C, implying that the rate controlling step of the reaction remains the same for the range of conditions investigated. Langmuir-Hinshelwood mechanisms, which could account for the observed non-elementary reaction order, however, typically would predict a change in the rate controlling step for such a range of conditions, and thus a shift in the observed order and overall activation energy. An appropriate mechanism for these data, therefore, requires an explanation of the reaction order (and activation energy) that remains largely invariant over a broad range of conditions. The observed reaction order is near enough to unity that the rate determining step in the reaction mechanism presumably involves oxygen adsorption at an active site. We propose a kinetic model that can be described in terms of the following steps:



where C_i is a free site with energy i ; $C(O)_i$ is an occupied site of energy i ; and CO_2 and CO the reaction products. Equation (3) is representative of reactions occurring at various edge sites. Oleksy¹² has specified the appropriate stoichiometry for edge sites of arm-chair, zig-zag, or mixed configurations¹³ for different surface complex coverages. Both CO and CO_2 are possible reaction products in these reactions. However, it is not possible at present to identify individual kinetic parameters for the various types of sites, and as a

result, we have chosen to represent these parallel reactions in terms of a continuous energy distribution function¹⁴. This approach decreases the number of parameters necessary to characterize the parallel set of reactions represented by (3). Reactions (2) and (4) are also assumed to occur at sites of different energies, and it is assumed that the rate equation for these reactions can also be expressed in terms of a continuous site energy distribution. However, it is assumed in the analysis that the parameter relating the site energy distribution to the activation energy for reaction at a site (i.e., the Polanyi relationship between the activation energy and the site energy) is not the same for each elementary reaction since each reaction step does not involve a common reaction intermediate (i.e., transition state).

At low temperatures (<850K) reaction (3) is assumed to be the rate controlling step in the mechanism. Transient kinetic measurements show that neither reaction (2) or (4) have activation energies or rates comparable to that of the gasification reaction. The rate controlling Eley-Rideal step proposed here for this reaction is in agreement with the work of Chen and Back¹⁵ and more recently Ahmed and Back¹¹, who have previously proposed this to be the principal rate controlling step in the low temperature oxidation mechanism. Ahmed and Back provided some direct evidence for this mechanism by showing that carbon gasification occurred only subsequent to the formation of surface oxides. In this study, the gasification of labile carbon atoms during the initial formation of the surface oxides made it impossible to separate the steady state carbon gasification rate from the measured carbon weight loss. However, we argue in favor of this mechanism as follows. The formation of CO from a surface complex requires approximately 70 kcal (in our calculations we have attributed ca. 20 kcal to a carbon surface energy, and have assumed the formation of a ketone bond between the oxygen atom and edge carbon), which is some 30 kcal greater than the measured overall activation energy of 40 kcal for the oxygen-Spherocarb reaction. The additional energy needed for desorption can only be obtained from the energy released when oxygen is adsorbed on the carbon surface. Bond rearrangements and energy transfer leading to the desorption of a surface complex would most likely occur if adsorption occurred at or adjacent to the surface complex. Secondly, the nearly first order dependence of the rate on oxygen partial pressure clearly suggests that reactions such as (2) to be the rate controlling. At present, the 0.75 reaction order must be taken as an empirical value. The non-integer reaction order could possibly be explained as the result of interaction between the oxygen molecule and a surface complex.

Conclusions

1. The initial rate of oxygen chemisorption on a microporous carbon is rapid and characterized by an activation energy of a few kcal. The adsorption data can be linearized when plotted as amount adsorbed vs. $\ln(t)$. The surface oxides are stable and remain on the carbon at temperatures below ~900K.
2. Char reactivity appears to correlate with the initial amount of oxygen chemisorbed. For the unreacted Spherocarb, a turn-over number of 0.0061 sec^{-1} at 773K and 0.1 atm oxygen was obtained.
3. The oxygen to carbon ratio increases dramatically with carbon conversion; however, no comparable increase in the steady state reactivity of the carbon is observed. The

secondary O/C ratio is a function of carbon conversion alone and independent of the particular reaction conditions.

3. The reaction order with respect to oxygen for Sphero carb is 0.75 and remains invariant over a broad range of oxygen partial pressure and temperature, implying that the rate controlling step in the reaction remains the same. Because the reaction order is near unity, it is proposed that the principal rate controlling step of the reaction involves the reaction of an oxygen molecule with a free site at a surface complex. It is proposed that the non-integer reaction order can be explained as the result of induced heterogeneity at a surface complex.

Acknowledgement

Acknowledgement is made to the donors of the Petroleum Research Fund, administered by the ACS, and to the University of Illinois for support of this research.

References

1. Marsh, H., in "Oxygen in the Metals and Gaseous Fuels Industries", Chemical Society, London (1978).
2. Essenhigh, R.H., in "Chemistry of Coal Utilization," Second Supplementary Volume, M. A. Elliott, ed., Wiley, New York (1981).
3. Laurendeau, N. M. Prog. Energy Combust. Sci. 4, 221 (1978)
4. Ahmed, S., Back, M.H., and Roscoe, J. M., Comb. and Flame 70,1 (1987).
5. Hurt, R. H., Dudek, D. R., Longwell, J. P., and Sarofim, A.F., "The Phenomenon of Gasification Induced Carbon Densification and its Influence on Pore Structure Evolution", to appear in Carbon, 1988.
6. Floess, J. K., Eden, G., and Lubarda, J., "Reaction-Diffusion Model of Microporous Carbon", Final report submitted to the Campus Research Board, University of Illinois at Chicago (1987).
7. Chihara, K., Suzuki, M., and Kawazoe, K., J. Colloid Interface Sci., 64, 584 (1976).
8. Everett, D. H. and Powl, J. C., J. Chem Soc., Faraday Trans. I, 619 (1976).
9. Gavalas, G., AIChE J. 26 577(1980).
10. Tucker, B. G. and Mulcahy, M. F. R., Trans. Faraday Soc. 65 274 (1969).
11. Ahmed, S. and Back, M.H., Carbon 23, 513 (1985).
12. Oleksy, S. A., MS Thesis, Department of Chemical Engineering, University of Illinois at Chicago (1988).
13. Ben-Aim, R. I., Int. Chem. Eng., 27, 70 (1987).
14. Boudart, M. and Djega-Mariadassou, G., "Kinetics of Heterogeneous Catalytic Reactions", Princeton University Press, Princeton, NJ (1984).
15. Chen, C-J. and Back, M. H., Carbon 17 495 (1979).

Table 1. Physical Properties and Chemical Composition of Spherocharb.

<u>Elemental Analysis</u>		Surface area	1020 m ² /g			
C	96.8 wt%	Micropore volume	0.39 cm ³ /g			
H	0.73 wt%	Pore radius ^a	6.7 Å			
O	2.43 wt%	Pore radius ^b	2.2 Å			
ash		~200 ppm				
<u>Conversion (%)</u>		0	20	40	60	80
Surface area (m ² /g-remaining)		1020	870	765	670	570

a. by application of the random pore model

b. from isosteric heat of adsorption

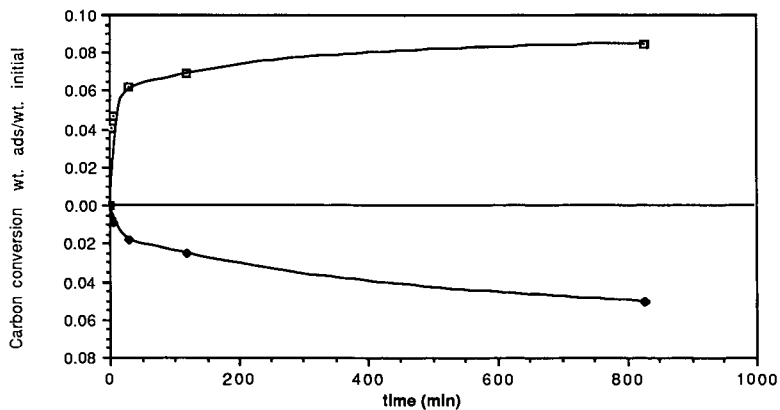


Figure 1. Adsorption and conversion curves at 563K and 0.5 atm; partially reacted Spherocharb.

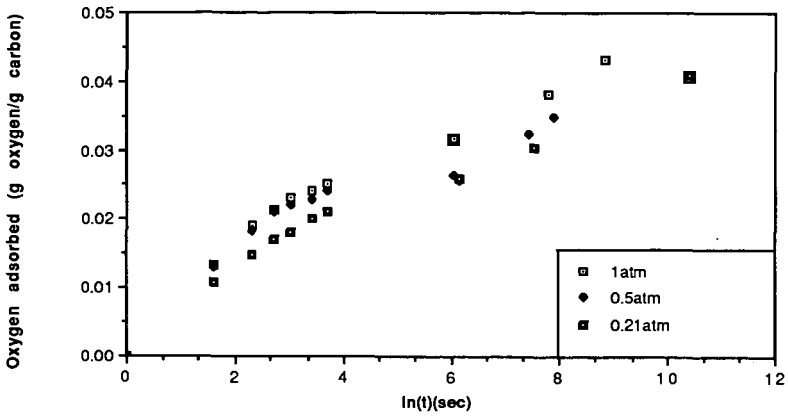


Figure 2. Oxygen adsorption vs ln(time) at 498K; partially reacted Spherocarb

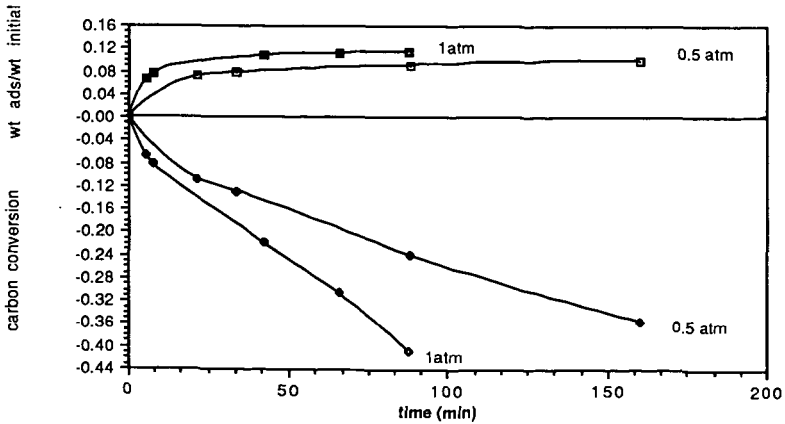


Figure 3. Adsorption and conversion curves at 708K for partially reacted Spherocarb (0.5 and 1 atm oxygen)

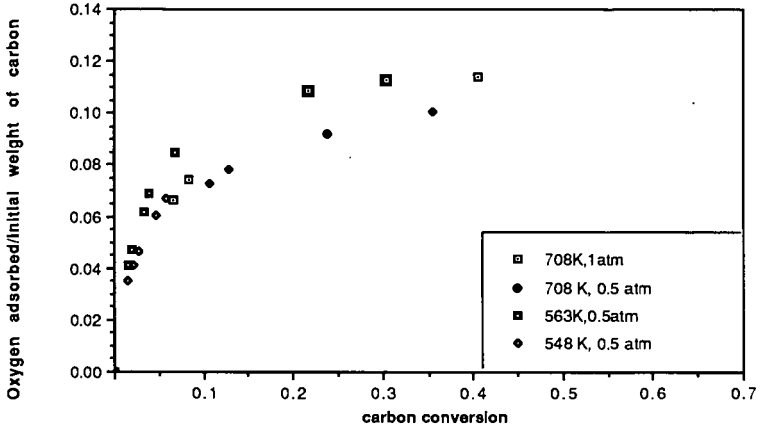


Figure 4. Amount of chemisorbed oxygen vs carbon conversion for the partially reacted Spherocharb.

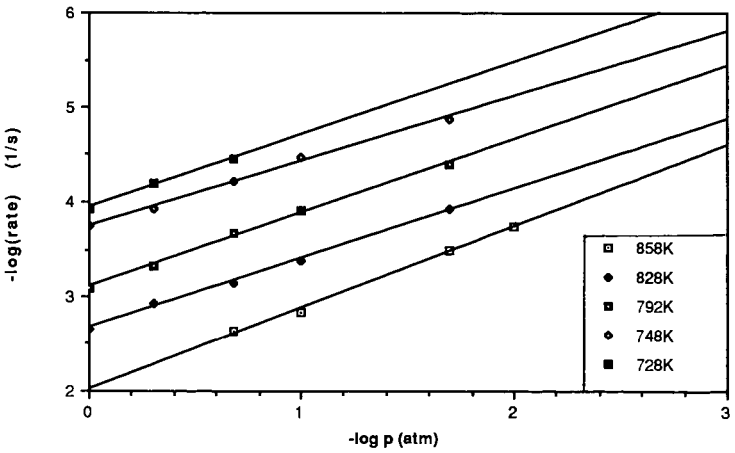


Figure 5. Variation of reactivity of Spherocharb with pressure.